Synthetic Interface Peptides as Inactivators of Multimeric Enzymes: Inhibitory and Conformational Properties of Three Fragments from *Lactobacillus casei* Thymidylate Synthase†

Variath Prasanna,‡,§ Surajit Bhattacharjya,‡ and Padmanabhan Balaram*,‡,§

Molecular Biophysics Unit, Indian Institute of Science, and Chemical Biology Unit, Jawaharlal Nehru Centre for Advanced Scientific Research, Bangalore 560012, India

Received August 22, 1997; Revised Manuscript Received December 22, 1997

ABSTRACT: Three synthetic peptides corresponding to distinct segments of the subunit interface of the dimeric enzyme thymidylate synthase (residues 17−38, N 22; residues 174−190, M 17; and residues 201−220, C 20) have been investigated for their ability to function as inhibitors by modifying the quaternary structure of the enzyme. A dramatic reduction of enzyme activity is observed following incubation of TS with the C 20 peptide. The N 22 and M 17 peptides were unable to cause any loss of enzymatic activity. Addition of the C 20 peptide results in a loss of fluorescence of TS labeled with a dansyl group at Cys 198, following aggregation and precipitation of the protein. The effects are not observed for the N 22 or M 17 peptides. Loss of enzymatic activity is related to the ability of C 20 to promote protein aggregation. The conformations of the peptides have been studied using CD and NMR in order to correlate the observed function with solution structures. Peptides N 22 and M 17 are largely unstructured in aqueous solution. A population of nascent helical structures or multiple turn conformations has been detected for the C 20 peptide in aqueous solution by NMR. Addition of 50% (v/v) hexafluoroacetone trihydrate (HFA), a structure-stabilizing cosolvent, stabilizes the helical conformation in the C 20 peptide. Under similar conditions, N 22 and M 17 remain largely extended with observations of local β-turn conformations. Interestingly, the C 20 peptide is a β-hairpin in the native structure, whereas the other two peptides are individual strand components of a β-sheet.

Thymidylate synthase (TS)[1] is a homodimeric enzyme which catalyzes the reductive methylation of deoxyuridine monophosphate (dUMP) to deoxythymidine monophosphate (dTMP) which is an essential precursor for DNA synthesis (*1*). Biosynthesis of dTMP using TS is the sole route in all living organisms, making the enzyme a key target for cancer chemotherapy (*2*, *3*). Inhibition of TS by fluorinated substrate-based analogues such as fluorinated deoxyuridine monophosphate (FdUMP) is a classical example of mechanism-based inhibition of enzyme action (*4*−*7*). Most recent work on TS inhibition has focused on the active site or cofactor binding site (*8*, *9*). We have undertaken an analysis of the utility of TS dimer interface peptides as potential inhibitors. The crystal structures of TS from diverse sources, *Lactobacillus casei* (*10*), *Escherichia coli* (*11*), *Leishmania major* (*12*), and human (*13*), reveal that the active site of the enzyme is constituted by residues from both subunits. The construction of an active site by contribution from residues on the two independent subunits has been elegantly demonstrated in complementation experiments involving site-specific inactivating mutants (*14*, *15*). Therefore, any kind of perturbations in quaternary association or in the dimer interface region of the enzyme might interfere with activity. The highly conserved nature of enzyme active sites precludes an effective distinction between host and target (pathogens or malignant cells) enzymes, requiring site-specific delivery strategies. In the case of multimeric enzymes, an alternative approach to inhibition would be to disrupt subunit assembly. The greater variability of protein−protein interfaces may permit efficient differentiation between host and target enzymes (*16*). Previous studies have shown that in HIV protease and ribonucleotide reductase, interface peptides are indeed potent inhibitors of multimeric enzymes (*17*−*20*). In this paper, we describe the inhibitory and conformational properties of three interface peptides, encompassing residues 17−38 (N 22), 201−220 (C 20), and 174−190 (M 17). The dimer interface of TS is predominantly formed by interaction between two six-stranded β-sheet structures (*21*, *22*). The N 22 and M 17 peptides are extended strand components of the β-sheets, whereas the C 20 peptide forms a β-hairpin conformation in the native structure of TS. The structural characterization of the peptides permits correlation of

† This work was supported by the Council of Scientific and Industrial Research, India.

* Address correspondence to the author at the Molecular Biophysics Unit, Indian Institute of Science, Bangalore 560012, India. Fax: 91-80-3341683. E-mail: pb@mbu.iisc.ernet.in.

‡ Molecular Biophysics Unit, Indian Institute of Science.

§ Chemical Biology Unit, Jawaharlar Nehru Center for Advanced Scientific Research.

[1] Abbreviations: TS, thymidylate synthase; CD, circular dichroism; NMR, nuclear magnetic resonance; IAEDANS, 5-[[2-(iodoacetyl)-amino]ethyl]amino]naphthalene-1-sulfonic acid; β-ME, 2-mercaptoethanol; DTT, dithiothreitol; EDTA, ethylenediaminetetraacetic acid; HFA, hexafluoroacetone hydrate or hexafluoropropane-2,2-diol; dUMP, deoxyuridine monophosphate; FdUMP, fluorodeoxyuridine monophosphate; MTHF, methylenetetrahydrofolate, TES, *N*-[tris(hydroxymethyl)methyl]-2-aminoethanesulfonic acid.

S0006-2960(97)02098-9 CCC: $15.00
Published on Web 04/23/1998

conformations with inhibitory potencies and examination of the strand and hairpin structures in isolation as a model folding system. The detection of a well-defined conformation in fragments has been correlated with the occurrence of nucleation sites in the folding process (*23*). Since C 20 forms a β-hairpin nucleated by an Asp 8−Gly 9 type I′ β-turn, conformational analysis of the synthetic fragment assumes special interest in view of many recent studies of the isolated β-hairpin in solution (*24*−*28*).

Our results demonstrate an effective inhibition of the enzymatic activity of TS by the C 20 peptide, which promotes protein aggregation, whereas the N 22 and M 17 peptides do not cause any loss of activity. The conformations of the peptides are studied by CD and 2-D NMR methods in aqueous solution and in aqueous hexafluoroacetone (HFA), a structure stabilizing cosolvent (*29*, *30*; Bhattacharjya et al., submitted for publication). Interestingly, the peptide C 20 adopts a nascent helical or multiple turn conformation in aqueous solution, whereas the other two peptides are largely unstructured under such conditions. The helical structure of C 20 is stabilized in a 50% (v/v) water/hexafluoroacetone mixture. On the other hand, the conformations of the N 22 and M 17 peptides were predominantly extended with evidence of local turns in 50% HFA.

MATERIALS AND METHODS

Ultrosyn KA resin, all Fmoc side chain protected pentafluorophenyl active esters, dimethylformamide (DMF), piperidine, 1-hydroxybenzotriazole, and trifluoroacetic acid (TFA) were purchased from Pharmacia (Sweden). Hexafluoroacetone trihydrate (HFA, a covalent hydrate of the ketone, a *gem*-diol, hexafluoropropane-2,2-diol) was obtained from Aldrich Chemical Co. dUMP, FdU-MP, and DTT were procured from Sigma Chemical Co., St. Louis, MO. All other chemicals were of analytical grade.

Peptide Synthesis. Peptides were synthesized on an LKB-Biolynx 4175 semiautomated peptide synthesizer using Fmoc chemistry. Side chain protecting groups were cleaved by treatment with 90−95% TFA in the presence of thioanisole (5%), anisole (2%), and ethanedithiol (5%) for a period of 4−6 h. The purity of the peptides were checked on an analytical HPLC column using a linear gradient of 80% acetonitrile/water containing 0.1% TFA. Peptides were characterized by electrospray mass spectrometry: C 20 (M_r calcd 2406.7, found 2406.3); M 17 (M_r calcd 2039.3, found 2038.8); and N 22 (M_r calcd for an *N*-acetyl derivative 2662.9, found 2662.5). Peptide N 22 was acetylated at the N-terminus following synthesis, before cleavage from the resin, due to contaminant acetic anhydride in acetic acid.

Activity Measurements. The activity of TS was measured by quantifying spectrophotometrically the conversion of tetrahydrofolate to dihydrofolate (*31*). Under standard conditions, an aliquot of TS (0.5−1 μg) was added to 1 mL of assay buffer consisting of 50 mM TES, pH 7.4, containing 25 mM $MgCl_2$, 6.5 mM HCHO, 1 mM EDTA, 75 mM β-mercaptoethanol (β-ME), 0.6 mM dUMP, and 0.15 mM MTHF. Following the addition of enzyme, the absorbance was monitored at 340 nm in a UV−visible spectrophotometer for a period of 4 min. The absorbance at the end of the stipulated time period was used to calculate the specific activity of the enzyme. To monitor the effect of the interface peptides on TS activity, the enzyme was incubated with the three peptides at various concentrations for a period of 1 h in 25 mM phosphate buffer, pH 6.9, containing 1 mM DTT, 0.1 mM EDTA at 25 °C before measuring the activity under standard conditions. The peptides were dissolved in water, and their concentrations were measured using the molar extinction coefficient values for Tyr and Trp at neutral pH (*32*) and of pure TS using a molar extinction coefficient value of 1.07×10^{-5} (*33*).

Fluorescence Measurements. TS was dansylated specifically at the active site Cys 198 residue using 5-[[2-[(iodoacetyl)amino]ethyl]amino]naphthalene-1-sulfonic acid (IAEDANS) according to protocols described elsewhere (*34*, *35*). The fluorescence of dansylated TS was monitored in the presence and absence of interface peptides in a Hitachi spectrofluorimeter with a band-pass of 5 nm for both the excitation and emission wavelengths. Samples were excited at 340 nm, and the emission spectrum was scanned between 380 and 560 nm. In separate experiments, dansylated TS was incubated with various concentrations of interface peptides over a period of 1 h at 25 °C. Following centrifugation at 5000 rpm for 1 min, the fluorescence intensity of the supernatant was measured.

Circular Dichroism (CD). All CD spectra were recorded on a JASCO-J-500A spectropolarimeter using a cell of path length 1 mm. The peptide concentrations for CD measurements ranged from 80 to 100 μM. In water, spectra were recorded at pH 3.5. The pH of the samples was ∼3.0 after addition of HFA as a cosolvent to aqueous solutions.

NMR Spectroscopy. ^{1}H NMR spectra were recorded on a Bruker AMX 400 spectrometer. The NMR spectra were recorded either in 90% H_2O/10% D_2O or in 40% H_2O/10% D_2O/50% HFA. The pHs of all the samples were adjusted to 3 by addition of 0.1 M HCl. A set of 1-D experiments were done at various concentrations and temperatures to test the aggregation properties of the peptides. Resonance assignments were performed using 2-D TOCSY, NOESY, and double quantum filtered COSY experiments. 2-D data were acquired at three different temperatures (295, 305, and 310 K) to obtain the complete resonance assignments. The peptide concentrations were fixed at 3.5 mM. NOESY experiments were done using a mixing time of 300 ms. A 70 ms mixing time was used for the TOCSY experiments. The residual water was suppressed by presaturating the water using a 55 dB pulse in a recycle delay of 1.5 s. The chemical shifts were with reference to sodium 3-(trimethylsilyl)-propionate-d_4 (TSP). All the 2-D data were acquired at 1K × 512 data points with 40−72 transients using a 5000−5500 Hz spectral width. 2-D data were zero-filled to 1K × 1K data points; the FIDs were multiplied by the sine $\pi/4$ function prior to Fourier transformation. Resonance assignments are provided as Supporting Information (Tables S1−S3).

Determination of NMR Constraints. Depending on the cross-peak intensities, the NOEs were classified into three different distance categories: strong, 2.0−3.0 Å; medium, 2.5−3.5 Å; and weak, 3.5−4.5 Å. In case of overlap, pseudoatoms were used allowing 1 Å relaxation in distance criteria. All the backbone to backbone, backbone to side chain, and side chain to side chain NOEs were considered. The dihedral angles (ϕ), used as constraints, were calculated

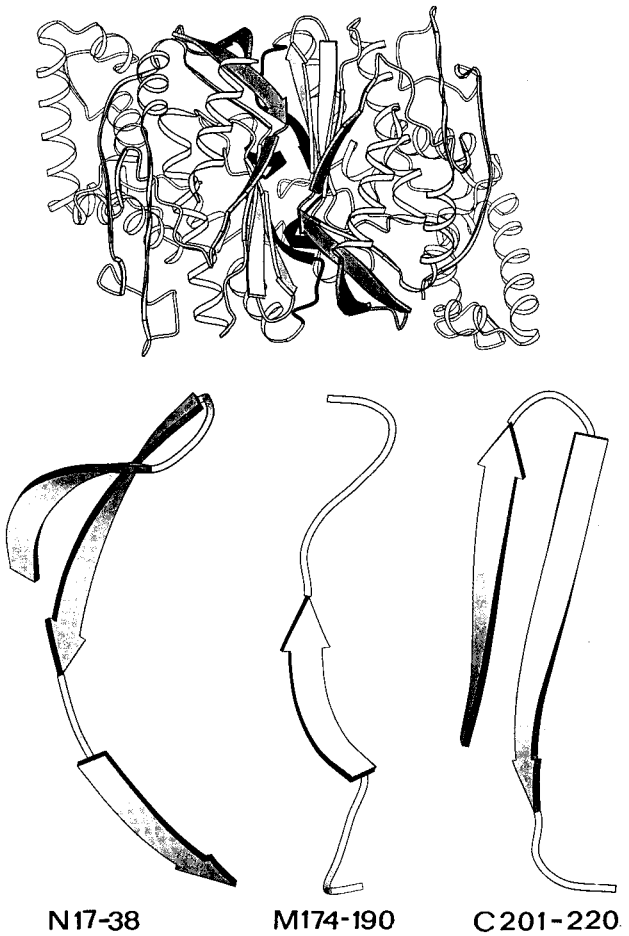

FIGURE 1: (Top) Ribbon drawing of *L. casei* thymidylate synthase showing both subunits prepared using MOLSCRIPT (*81*). The peptides at the interface (from the two six-stranded β-sheets) (N 22, M 17, and C 20) are colored black, medium gray, and light gray, respectively. The coordinate set 4tms from the Brookhaven Protein Data Bank (*10*, *11*) has been used to generate the ribbon diagram. (Bottom) Native structures of the three interface peptides.

from $^3J_{NH\alpha}$ using a modified Karplus type equation (*36*) and an empirical relationship given by Wishart et. al. (*37*) relating the chemical shift deviation of the $C^{\alpha}H$ proton and the dihedral angle ϕ: $\Delta\delta = -0.013\phi - 1.20$, where $\Delta\delta$ is the deviation of the chemical shift of $C^{\alpha}H$ from its random coil value. The spectral overlap precluded determination of J for all the residues. In such cases, we have calculated ϕ using the above relationship. ϕ values obtained using both methods vary only by $\pm 10°$.

Structure Calculation. All the computations were performed on an Iris Silicon Graphics workstation using the INSIGHT II molecular modeling program. The CVFF force field was used for energy minimization, and molecular dynamics simulations (MD) were carried out with the Discover module. A biharmonic skewed potential function was used in the total energy expression to include distance constraints. All the peptide bonds were maintained in a trans geometry throughout. A force constant of 10−20 kcal/mol was used on all constraints as a penalty function for violation of distance criteria. A few cycles of steepest descent energy minimization were done without any constraints to relax short contacts from the initial structures. Different starting structures were used from extended to helical conformations for structure calculation with imposed constraints. The dihedral angles Ψ for the first residue and Φ for the last residue were fixed at 180° in the starting structure. The constrained MD simulations were performed at 300 K for 200 ps with a 25 ps equilibration period. All the constraints were not imposed together. The short-range distance constraints were used to generate an initial set of structures, which were further refined by medium NOE distances. The geometry of the structures and the restraint violations were examined in each step of simulation. A set of 25 structures were generated of which 15 structures showed low rms deviation from the average structure. The 'stereochemical goodness' of the 15 different structures was evaluated by calculating the ϕ, ψ dihedral angles.

N 22 : G-H-F-K-P-D-R-T-H-T-G-T-Y-S-I-F-G-H-Q-M-R-F

M 17 : H-P-Y-S-R-R-L-I-V-S-A-W-N-P-E-D-V

C 20 : L-Y-Q-F-Y-V-N-D-G-K-L-S-L-Q-L-Y-Q-R-S-A

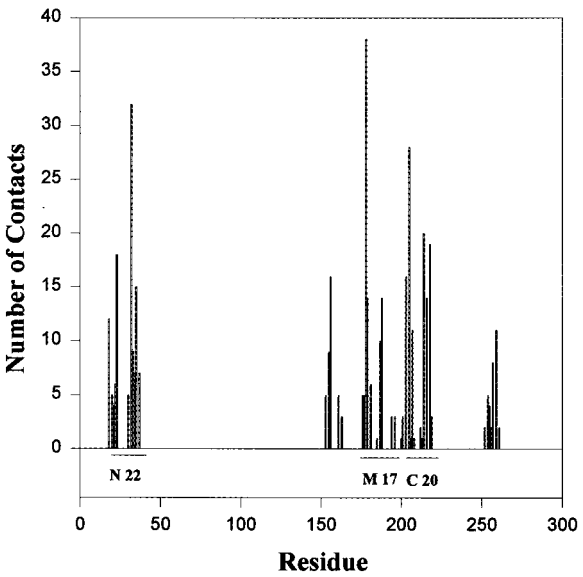

FIGURE 2: Bar diagram indicating intersubunit contacts at the interface region of thymidylate synthase. A contact distance between nonbonded atoms on the two subunits of <4 Å defines an intersubunit atom−atom contact. The amino acid sequences of the three selected peptides (N 22, M 17, and C 20) encompassing the maximum zone of contacts are also shown.

RESULTS

Selection of Peptides from the Dimer Interface of TS. The dimeric structure (*10*) of TS from *L. casei* is shown in Figure 1. The peptides are chosen depending on the number of contacts made by the residues between the two subunits, based on the premise that maximum contact zones will yield peptides of higher complementing activity. A contact plot (Figure 2) mapped three major segments comprising residues 17−38 (GHFKPDRTHTGTYSIFGHQMRF) (N 22), 174−190 (HPYSRRLIVSAWNPEDV) (M 17), and 201−220 (LYQFYVNDGKLSLQLYQRSA) (C 20) covering almost the entire region of the linear polypeptide chain encompassing the dimer interface. These segments were selected for our studies. Table 1 compares the contribution made by the three interface segments to the buried surface area of the subunits on dimerization. In *L. casei* TS, 2368 $Å^2$/subunit

Table 1: Accessible Surface Area (ASA, Å^2) for the Interface Peptides in Thymidylate Synthase[a]

	ASA values (Å^2)		
	N 22	M 17	C 20
isolated fragment	2850	2419	2403
fragment in monomer	1554	1262	787
fragment in dimer	909	456	271
Δ ASA (ASA of fragment in monomer − ASA of fragment in dimer)	645	806	516
ASA (%) buried upon dimerization	22.6	33	21
contribution (%) of each fragment to interface (A_i)	27	34	21.7

[a] The ASA (accessible surface area) values have been obtained from the structure of *L. casei* TS (PDB code 4tms). The ASA values for the isolated fragments are determined for each peptide with its secondary structure intact as in native TS. The ASA values for the fragments in the monomer and dimer are obtained when their structure is part of the folded crystallographic monomer and dimer, respectively. Δ ASA represents the buried surface area per subunit. A_i is the ratio of the buried surface area of each segment with respect to the total buried surface area at the interface. A total of 2368 Å^2/subunit surface area is buried at the interface of TS.

area is buried upon dimer assembly. An analysis of 32 homodimeric proteins of known crystal structures reveals that the buried surface area per subunit ranges from 368 to 4746 Å^2 with a mean value of 1685 Å^2 (*38*). The percentage accessible surface area buried upon dimerization is 15.35% of the monomer surface area in TS. This may be compared with a value of 27% for the HIV protease dimer which has been successfully targeted using interface peptides (*39*). The three interface peptides make comparable contributions to the dimer interface in terms of the buried surface area, with M 17 making a marginally larger contribution than the other two peptides. The presence of charged (R, K, D, E, H), neutral and polar (G, S, T, Q, N, Y, C), and hydrophobic residues (W, F, I, L, V, P, M) at a distance of 4 Å or less from an atom across the subunit was examined. The following distributions (%) were obtained: N 22, charged 55, polar 27, hydrophobic 18; M 17, charged 37.5, polar 25, hydrophobic 37.5; C 20, charged 11.1, polar 77.7, hydrophobic 11.1. The TS interface reveals several polar interactions involving hydrogen bonds and potential salt bridge formation, a feature reminiscent of other interfaces which generally appear to be significantly more polar than protein interiors (*40*, *41*).

Enzymatic Assay of TS in the Presence of the Peptides. The catalytic activity of native TS is independently measured with the three interface peptides (N 22, M 17, and C 20). Peptides at varying concentrations are incubated with TS in phosphate buffer, pH 6.9 at 25 °C (see Materials and Methods), and aliquots of the enzyme assayed for activity under standard conditions. Figure 3 clearly demonstrates a dramatic loss of enzymatic activity of TS by the peptide C 20. The peptide-mediated inhibition is concentration dependent, and a 95−100% inhibition of enzymatic activity is observed at 250−300-fold molar excess of C 20. The IC_{50} value of C 20 is calculated to be 18 μM, which corresponds in these experiments to a 120-fold molar excess of peptide over the enzyme. On the other hand, the N 22 and M 17 peptides are virtually inactive; preincubation of TS even in 1000-fold molar excess of either N 22 or M 17 under identical conditions does not yield any significant change in enzymatic activity (Figure 3). The enzymatic inhibition of

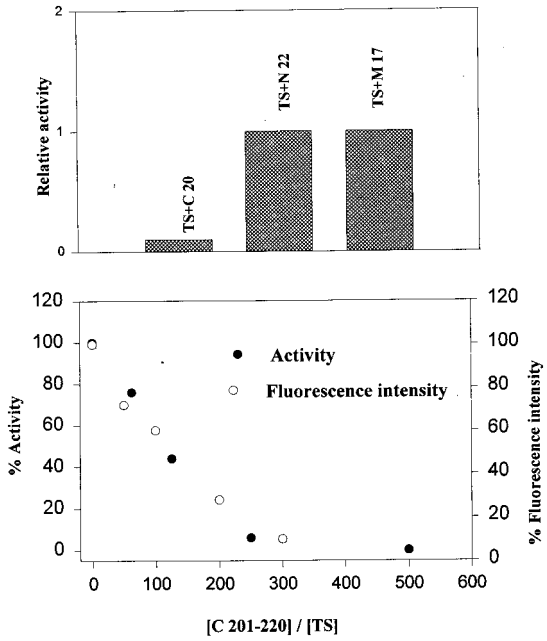

FIGURE 3: (Top) Bar diagram showing loss of enzymatic activity of TS in the presence of the interface peptides. 0.14 μM TS was incubated with 28 μM peptide C 20 and 141 μM peptides N 22 and M 17 for 1 h at 25 °C in phosphate buffer, pH 6.9, containing 1 mM DTT, 0.1 mM EDTA before measuring the activity under standard conditions. The ordinate represents the relative activity of TS in the presence and absence of peptide. (Bottom) Plot showing decrease in enzymatic activity and fluorescence intensity of dansylated TS as a function of C 20 concentrations. 0.14 μM TS was incubated with 62.5−500-fold molar excess (8.8 μM−70 μM) of peptide C 20 1 h at 25 °C in phosphate buffer, pH 6.9 containing 1 mM DTT, 0.1 mM EDTA before measuring the activity under standard conditions. Dansylated TS (0.14 μM) was likewise treated, and after 1 h of incubation, the samples were centrifuged for 1 min at 5000 rpm and the fluorescence of the dansyl group in the residual protein was measured at 25 °C.

TS by the C 20 peptide is highly specific since it does not inhibit other unrelated, multimeric (or dimeric) enzymes such as triosphosphate isomerase (TIM) or serine hydroxymethyl transferase (SHMT) (data not shown).

Mode of Inhibition. To examine the structural changes of TS upon binding to its interface peptides, the fluorescence of dansylated TS has been monitored. The fluorescence of the extrinsic dansyl rather than the intrinsic tryptophan emission of TS has been monitored to avoid interference due to absorption/fluorescence of tyrosine and tryptophan residues of the peptides. The catalytic Cys 198 residue which resides at the dimer interface of TS has been labeled specifically. Therefore, any structural perturbations occurring around the interface region of the protein will be reflected in the fluorescence properties of the probe. There is a progressive diminution of the fluorescence intensity of IAEDANS with increasing concentrations of the C 20 peptide (Figure 4). The fluorescence spectra were unaffected in the case of M 17 and N 22 peptides under identical conditions (data not shown). The loss of enzymatic activity of TS coincides well with the quenching of IAEDANS fluorescence (Figure 3). The loss of fluorescence intensity clearly demonstrates a direct and, more importantly, specific interaction of the C 20 peptide with TS, whereas the other two peptides which are unable to inhibit the enzymatic activity are also without effect on IAEDANS fluorescence. The quenching of fluorescence intensity can arise from dynamic

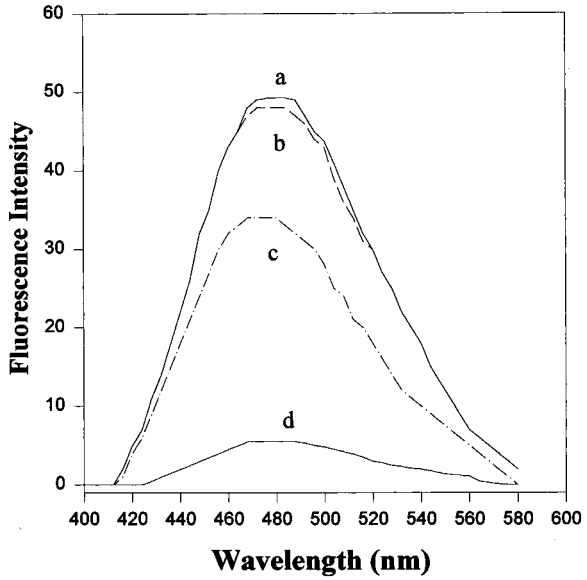

FIGURE 4: Fluorescence emission spectra of IAEDANS-labeled TS (0.14 μM) in the presence of various molar excess of the C 20 peptide: (a) 0 μM, (b) 2.8 μM, (c) 7.0 μM, (d) 28.0 μM in phosphate buffer, pH 6.9, containing 1 mM DTT and 0.1 mM EDTA. Samples were excited at 340 nm, and the emission spectrum was scanned between 380 and 560 nm.

collision of the peptide with the chromophore or loss of protein from the solution due to precipitation. The C 20 peptide inhibits TS activity as a result of protein aggregation with the formation of a gel-like precipitate, upon incubation of TS with peptide. The parallel loss of enzymatic activity of TS and fluorescence intensity supports the fact that protein aggregation appears responsible for peptide-induced inhibition. To explore the possible synergy in the action of the interface peptides, the effect of C 20 on TS activity was studied in the presence of the other two peptides, (N 22 and M 17, individually and in combination. Even at high peptide concentration (350 μM), no effect on C 20-induced inhibition was observed (data not shown).

Conformational Characterization. (A) CD Studies. Figure 5 summarizes CD studies of the three peptides in aqueous solution, pH 3.5, in 20 mM phosphate buffer, pH 6.9, and in 50% HFA/water mixture, pH 3.0. In aqueous solution, the N 22 and M 17 peptides lack appreciable secondary structure, yielding a single negative CD band at 200 nm. The CD spectra are unaffected by variation in salt concentration and pH. The CD spectra of the C 20 peptide in water at low pH and in phosphate buffer are supportive of a significant population of structured species. A negative CD band at ~212 nm could be interpreted as arising from multiple β-turns or a β-hairpin conformation (*42*). We have recently observed that an HFA like 2,2,2-trifluoroethanol (TFE) stabilizes helical structures in diverse peptide sequences and is indeed a more potent structure inducer (*29*). The induction of helicity by fluoroalcohols depends on the intrinsic propensity of the peptide sequences to adopt helical conformations (*43*, *44*). A remarkable structural transition to a helical conformation is observed in the case of the C 20 peptide in HFA. CD spectra recorded in a 50% HFA/water mixture reveal a characteristic helical spectrum with minima at ~222 and 202 nm. On the other hand, CD spectra remain unchanged in the M 17 peptide in 50% HFA, indicating the absence of induction of any secondary structures. A

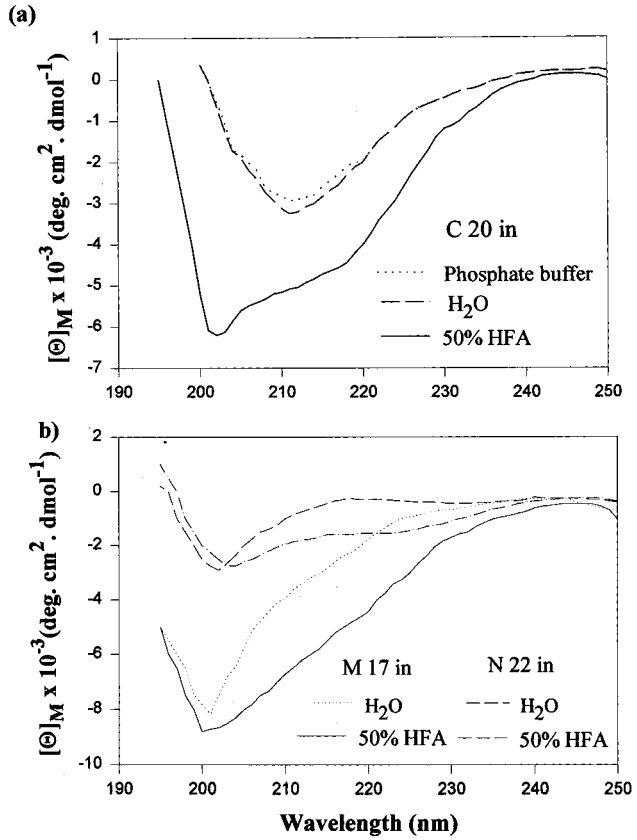

FIGURE 5: Far-UV CD spectra of the C 20 (top), M 17 and N 22 (bottom) peptides in 25 mM phosphate buffer, pH 6.9, in aqueous solution, pH 3.5, and in 50% HFA, pH 3.0 The concentrations of the peptide samples were in the range of 80−100 μM. A path length of 1 mm was used throughout all the experiments.

relatively small increase in absorption at ~222 nm is also observed in the N 22 peptide, in 50% HFA/water, presumably indicating stabilization of some helical structure. However, it is to be noted that the N 22 peptide contains a large number of aromatic residues (three histidine, three phenylalanine, and one tyrosine) which might contribute to the far-UV CD bands (*45*, *46*). The CD spectra of N 22 in aqueous solution do indeed show a broad shallow band in the region of 220−230 nm, suggesting possible contributions from the aromatic residues. NMR studies of the N 22 peptide in aqueous solution and in 50% HFA indicate a largely nonhelical conformation (vide infra).

(B) NMR Studies. (i) Conformations of the C 20 Peptide in Water and in 50% HFA/H_2O. Earlier investigations had indicated that potential β-sheet peptides have a strong tendency to aggregate in solution (*23*, *47*, *48*). We have examined the aggregation of the three interface peptides by dilution experiments. 1-D NMR spectra of C 20, N 22, and M 17 were recorded at various concentrations, ranging from 1 to 5 mM. The line widths and chemical shifts of the amide protons and aromatic ring proton resonances were identical throughout the concentration range, indicating the absence of aggregation (data not shown).

Resonance assignments and structure determinations were performed following standard procedures using 2-D TOCSY, dQF-COSY, and NOESY experiments (*49*). The "native like" β-hairpin conformation of the C 20 peptide does not exist in aqueous solution. There are no long-range interstrand or $C^{\alpha}H/C^{\alpha}H$ NOEs, characteristic of β-sheet or

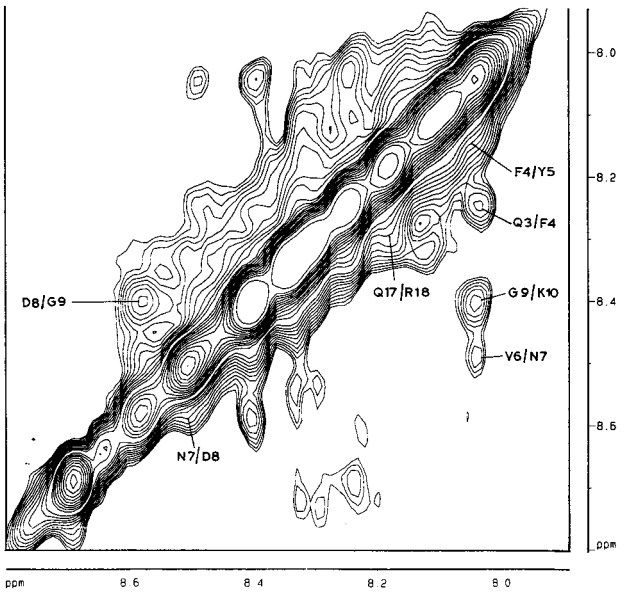

FIGURE 6: Partial 2-D NOESY spectrum of peptide C 20 in aqueous solution at pH 3.0, 295 K indicating NH/NH NOEs. The concentration of the peptide was typically 3.5 mM. The spectra were recorded with a 300 ms mixing time.

β-hairpin conformations in the NOESY spectra of C 20 in water. However, observations of sequential C$^{\alpha}$H/NH NOEs throughout the peptide backbone indicate an extended conformation. Interestingly, the N terminus of the peptide shows weak sequential NH/NH NOEs from residues 3 to 10 indicating a population of folded conformations, with backbone ϕ, ψ values lying in the helical region (Figure 6). However, the medium-range NOEs (C$^{\alpha}$H/NH *i*, *i*+3; C$^{\alpha}$H/NH *i*, *i*+4; or C$^{\alpha}$H/C$^{\beta}$H *i*, *i*+3) which are diagnostic of stable helical conformations are absent. This kind of folded conformation has been referred to as a "nascent helix" or multiple turn structures (*50*). The chemical shifts of C$^{\alpha}$H protons are exquisitely sensitive to the conformation; an upfield or downfield shift in the C$^{\alpha}$H resonance from the random coil values is suggestive of either helical or β-sheet conformation, respectively (*37*, *51*). The chemical shift perturbations of C$^{\alpha}$H resonances of the C 20 peptide in water from random coil values are limited, suggesting the population of folded conformations is small (Figure 7).

Addition of HFA (50% v/v) dramatically stabilizes the helical conformations, as judged by intense sequential (i, i+1) NH/NH, C$^{\beta}$H/NH NOEs, and weak C$^{\alpha}$H/NH NOEs along with strong intraresidue C$^{\alpha}$H/NH NOEs (Figures 8, 9). The observations of many medium range NOEs (C$^{\alpha}$H/NH *i*, *i*+3; C$^{\alpha}$H/C$^{\beta}$H *i*, *i*+3) and NH/NH (*i*, *i*+2) NOEs are indeed suggestive of a stable helical conformation (Figure 9). Substantial deviations of C$^{\alpha}$H chemical shifts from the random coil values are also indicative of induction of helicity in a 50% HFA/water mixture (Figure 7). The presence of C$^{\alpha}$H/NH *i*, *i*+4 NOEs and the paucity of C$^{\alpha}$H/NH *i*, *i*+2 NOEs indicate an α-helical conformation of the C 20 peptide (Figure 9). The nascent helical conformation of C 20 in aqueous solution, which spans residues 3−10, is merely stabilized in HFA, with little extension toward the C terminus. The sequential NH/NH NOEs in C 20 in aqueous HFA start from Y 2 and continue up to L 13 with some interruptions due to spectral overlap. The observations of an NH/NH NOE between Q17/R18 and a C$^{\alpha}$H/NH (i, i+2) NOE between Q14/Y16 presumably indicate turn structures at the C terminus of the peptide.

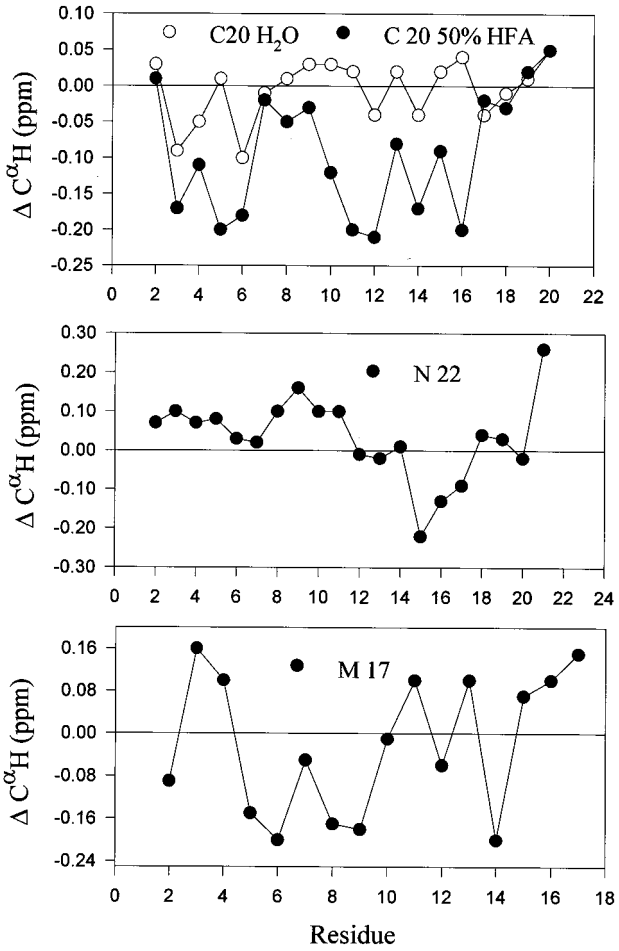

FIGURE 7: C$^{\alpha}$H chemical shift deviations of the peptides (C 20, M 17 and N 22) from random coil values in water and 50% HFA, pH 3.0.

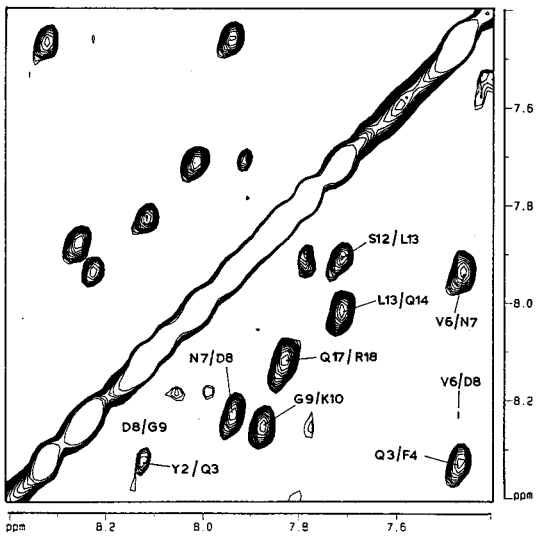

FIGURE 8: Partial 2-D NOESY spectrum of peptide C 20 in 50% HFA, at pH 3.0, 310 K, indicating NH/NH NOEs. The concentration of the peptides was 3.5 mM. The spectra were recorded with a 300 ms mixing time.

(ii) Structure of the C 20 Peptide. Observation of a large number of NOEs in 50% HFA permits determination of a reliable structure of the C 20 peptide using NMR constraints. Figure 10 shows a superposition of 15 constrained MD

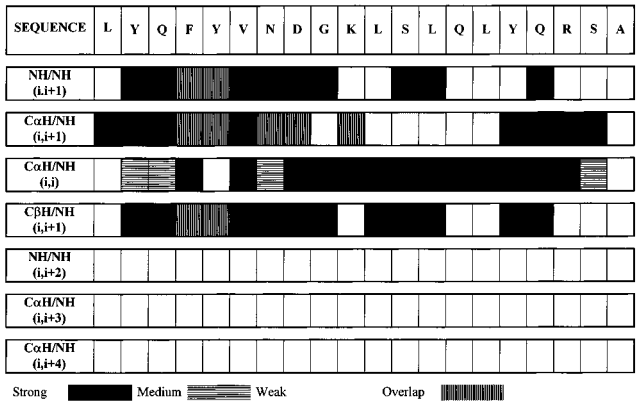

FIGURE 9: NOE summary for peptide C 20. The amino acid sequence is shown at the top. The intensities of the NOEs are categorized as either strong, medium, or weak and marked accordingly by different shades.

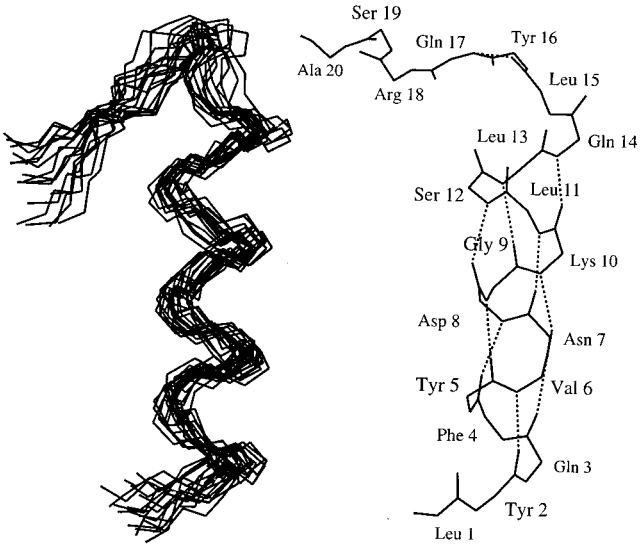

FIGURE 10: Superposition of the backbone atoms of 15 constrained MD simulated structures of peptide C 20. The structures superpose closely at the helical region of the peptide with a RMSD of 0.7 Å (right). The average conformation of peptide C 20 indicating the hydrogen bonds in the helical region (2−14) is presented (left).

simulated structures. A close superposition is evident for residues 2−14 which encompass the helical region of the peptide. The C terminal tail of the peptide (residues 15−20) is extended, exhibiting a greater motional freedom. The RMSD values for the backbone atoms (C^{α}, N, C′) are calculated to be 0.7 Å for the helical region (residues 2−14) and 1.2 Å for all the backbone atoms. The backbone dihedral angles (Φ, Ψ) are well inside the allowed region of the Ramachandran map (*52*), indicating 'stereochemical goodness' of the calculated structures. The Φ, Ψ values of the helical region of the peptide are well clustered around $60 \pm 15°$ and $45 \pm 10°$, respectively, whereas the other residues are in the extended regions of Φ, Ψ space.

(iii) Conformations of the N 22 and M 17 Peptides in Aqueous Solution. Both peptides do not show evidence for ordered conformations in water. The limited chemical shift dispersion (~0.5−0.6 ppm for $C^{\alpha}H$ and NH resonances) and the presence of few NOEs preclude detailed resonance assignments (data not shown). However, in the N 22 peptide, K 4 and a stretch of residues at the C-terminus, G 11−M 20, could be identified due to the presence of amino acids (I 15, S 10, Q 19, and M 20) with unique spin systems. The NOESY cross-peaks between the identified residues of N 22 are mainly characterized both by strong intraresidue $C^{\alpha}H$/NH and by sequential $C^{\alpha}H$/NH NOEs. The NOEs from backbone to side chains and from side chains to side chains are weak and few in number. The chemical shifts of many of the resonances are close to the random coil values (*49*). Taken together, these results suggest a dynamic averaging among an ensemble of conformations, with no preference for an ordered structure. The conformation of the M 17 peptide is also similar to N 22, with an even smaller dispersion of chemical shifts and a limited number of NOEs.

(iv) Conformations of the N 22 and M 17 Peptides in 50% HFA/Water. In aqueous HFA (50% v/v), larger dispersions in chemical shifts and several NOEs are obtained for both the peptides. Resonance assignments are achieved for all the residues in N 22 and M 17, with the exception of the terminal amino acids. The observations of strong to medium intensities for sequential $C^{\alpha}H$/NH and weak intraresidue $C^{\alpha}H$/NH NOEs throughout the peptide chain are suggestive of stabilization of a "native like" extended strand conformation of the N 22 peptide in 50% HFA (Figure 11). The chemical shifts of many of the $C^{\alpha}H$ resonances show a downfield shift as compared to their random coil values, indicating populations of stable extended β-strand conformations (Figure 7). However, the extent of downfield shifts is limited as compared to the downfield shifts observed for strands in β-sheet structures. The larger downfield shifts of the $C^{\alpha}H$ protons in the β-sheet structure result from interstrand hydrogen bonding and large deshielding due to the proximal carbonyl oxygen from neighboring strands (*37*). These effects are absent in isolated strands. However, the extent of the shift may be affected due to the occurrence of as many as seven aromatic residues in the N 22 sequence. The "ring current" effect of the aromatic residues may indeed reduce the extent of downfield shift of $C^{\alpha}H$ resonances, which are in close proximity to the aromatic ring. The C terminus of N 22 shows a population of "nonnative" multiple β-turn conformations, as judged by four sequential NH/NH NOEs from residues Q 19 to M 21. This is further supported by the presence of intense intraresidue $C^{\alpha}H$/NH NOEs as compared to the sequential $C^{\alpha}H$/NH NOEs in this region of the peptide. The observation of an NH/NH NOE between G 11/T 12, together with the presence of a $C^{\alpha}H$/NH NOE between T 10/G 11, suggests a type II β-turn with G 11 and T 12 at the $i+1$ and $i+2$ positions.

Analysis of the NOESY spectra of the M 17 peptide shows strong/medium sequential $C^{\alpha}H$/NH NOEs and weak intraresidue $C^{\alpha}H$/NH NOEs, suggesting an extended conformation (Figure 11). The M 17 peptide sequence has two Pro residues; the occurrence of cis/trans isomerization about the H 1−P 2 peptide bond complicates the NMR spectra, resulting in additional resonances. A weak $C^{\alpha}H/C^{\alpha}H$ NOE between H 1/P 2 indicates the existence of a minor cis conformation. The peptide bond around N 13/P 14 remains trans as judged by NH/$C^{\delta}H_2$ NOEs. The chemical shift deviation of the $C^{\alpha}H$ protons does not show any characteristic structural dependence, presumably due to the complications arising from the conformational exchange. In the native structure, the M 17 peptide contains two type I β-turns which are centered around P 14/E 15 and S 4/R 5. The type I β-turn at P 14/E 15 is formed in 50% HFA/H_2O solution. The

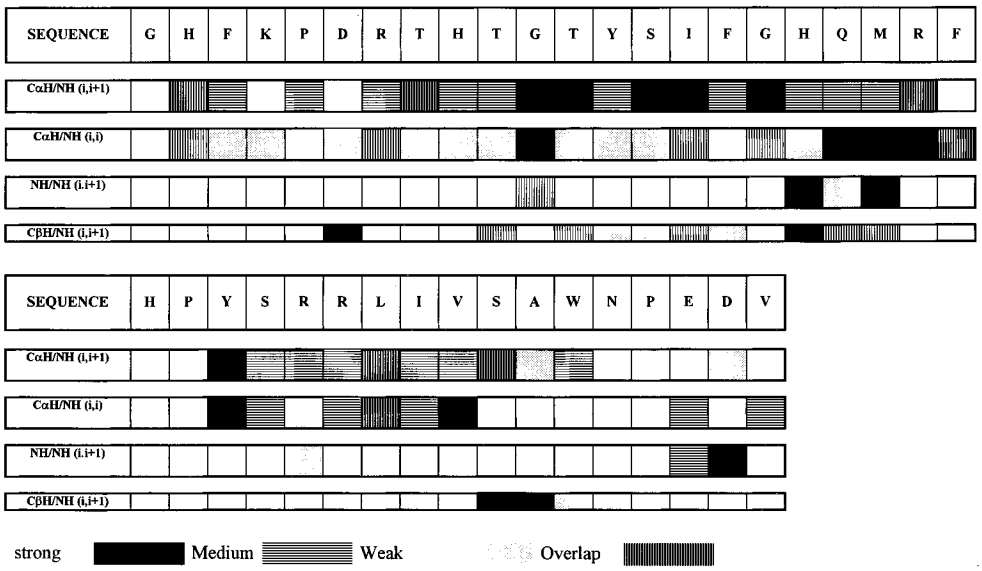

FIGURE 11: NOE summary for the peptides N 22 and M 17. The amino acid sequence is shown at the top. The intensities of the NOEs are categorized as either strong, medium, or weak and marked accordingly by different shades.

observations of an NH/NH NOE between E 15/D 16 and the absence of a P 14/E 15 $C^{\alpha}H$/NH NOE are indicative of the 'native like' β-turn. The presence of another NH/NH NOE between D 16/V 17 could also indicate a population of β-turns around E 15/D 16 at the C terminus. The NH/NH NOE (Figure 11) between R 5/R 6 is supportive of a 'native like' turn at that position.

DISCUSSION

The potential of interface peptides to inhibit the activity and assembly of oligomeric enzymes has been well documented (*17*, *19*, *20*, *39*, *53*, *54*). We have studied inhibition and conformational characteristics of three interface peptides from TS. Our results establish that the peptide derived from segment 201−220 of TS (C 20) does indeed possess appreciable inhibitory activity. The other two peptides, N 22 and M 17, do not cause any significant loss of enzymatic activity. The mechanism by which the C 20 peptide inhibits TS enzymatic activity is an outcome of aggregation and precipitation of TS from solution. Protein association has turned out to be a common feature following structural perturbation in multimeric enzymes including TS (*55*, *56*, *35*, *57*). Unfolding studies of TS in the presence of chemical denaturants (urea or guanidinium chloride) had previously identified a fragile region at the dimeric interface of the protein, which presumably 'catalyzes' the formation of soluble aggregates in a partially folded form of the protein (*35*). Reinforcement of the fragile region in the dimer interface, by covalent disulfide cross bridges, in an engineered TS mutant (T155C/E188C/C244T) abolished such an aggregation process (*58*). The C 20 peptide induced enzymatic inhibition and aggregation seems to be highly specific since the other two interface peptides, M 17 and N 22, neither cause any loss of activity nor precipitate TS. The C 20 peptide also does not facilitate any protein aggregation or inhibition in unrelated oligomeric proteins (TIM, SHMT). A specific conformation of TS indeed seems to be required for the binding of the peptide as demonstrated by the fact that the ternary complex of the enzyme (TS+FdUMP+MTHF) alone was found to be resistant to peptide-mediated aggregation and not the TS+FdUMP or the TS+MTHF complexes. This feature was noted in studies using an inhibitory analogue of C 20 which has Asp 8 replaced by a D-Pro residue (unpublished results). It is relevant to point out that substantial conformational changes have been demonstrated in the ternary complex of TS by crystallographic studies (*59*).

Conformational studies in solution suggest a correlation between peptide structure and inhibitory activity. Interestingly, segments lacking well-defined conformations (N 22 and M 17) do not inhibit the enzyme while the structured peptide C 20 is a good inhibitor. Ironically, the solution conformation determined for C 20 is nonnative. A population of folded conformations of the inhibitory C 20 peptide, resembling multiple β-turns or 'nascent helix' at the N terminal of the peptide, is established by CD and NMR in aqueous solution. On the contrary, the N 22 and M 17 peptides appear to be largely unstructured in water and have no detectable inhibition of TS activity. The nascent helical structure of the C 20 peptide is dramatically stabilized in 50% HFA solution, whereas the peptide is in a β-hairpin conformation in the native structure of TS. The detection of a nonnative conformation of the C 20 peptide in aqueous solution or in the presence of structure-stabilizing cosolvents and the role of such conformations in enzymatic inhibition are not easily rationalized. In aqueous solution, the peptide may exist as an ensemble of different conformations. The active conformation could be a minor species which has a 'native like' hairpin conformation. Alternatively, a nonnative conformation could indeed be responsible for promoting aggregation since protein association in the case of TS is facilitated by conditions which cause significant structural perturbations. To resolve this issue, structure−activity studies of different peptide analogues having substitutions with conformationally restricted amino acids to freeze desired conformations are required. It is well established that placement of D-Pro residues in the $i+1$ position of β-turns facilitates nucleation of β-hairpin conformations (*60*−*62*). A designed analogue replacing Asp 8 by D-Pro in the $i+1$ position of the β-turn in the C 20 is a good inhibitor of TS activity (unpublished results). It is likely that further

modifications of the C 20 peptide to stabilize specific folded conformations might yield a more potent inhibitor with a much higher affinity for the enzyme.

Lessons from Conformational Studies on Synthetic Protein Fragments. The observations of transient or stable structures in isolated peptides without any long-range interactions are directly correlated to their potential as 'nucleation sites' in protein folding (*23*, *63*). Peptide fragments comprising the entire sequence of proteins have been probed in aqueous or in aqueous/alcohol mixtures to establish sequences with stable secondary structure (*23*, *64*−*67*). Our results show that the three peptide fragments encompassing almost the entire dimer interface of TS have different conformational characteristics in aqueous solution and in water/HFA mixtures. The peptide C 20, which is a β-hairpin in the native protein, folds into a 'nascent helical' structure in H_2O. The helical conformation is stabilized upon addition of HFA. The formation of secondary structures by the peptide fragments in aqueous solution or in alcohol/water mixture depends on the intrinsic propensities of the amino acids (*68*, *69*, *64*). Recent studies demonstrate that Thr and Ile are among the amino acids which have very high β-sheet-forming propensities (*70*, *71*). The C 20 peptide sequence does not contain any Thr or Ile residues. However, the presence of residues such as Leu, Gln, or Lys which are known to favor helical conformations (*72*, *73*) presumably stabilizes the helical nonnative structure in the C 20 fragment. The probable roles of nonnative structures in the folding pathway of proteins have been demonstrated in many cases (*74*−*76*). In the folding pathway of TS, this peptide fragment C 20 may adopt a transient helical structure in the early stage of folding which in principle could transform into a nativelike conformation later in the folding process.

The N 22 and M 17 peptides are largely random coil in aqueous solution as judged by CD and NMR parameters. Addition of HFA does not result in any significant change in the CD spectra, but the NMR data are suggestive of a change in conformational characteristics. A nativelike extended conformation is observed for both the peptides, which also suggests that structure stabilization by HFA like other fluoroalcohols is strongly sequence dependent. The presence of many β-branched residues such as Thr, Ile, or Val presumably stabilizes the extended strand conformation in N 22 and M 17 peptides in HFA/water solution. The nativelike β-turn conformation around N 13 and P 14 in M 17 is preserved in 50% HFA. The remarkable ability of HFA and related fluoroalcohols to stabilize well-defined peptide folds is a consequence of their amphipathicity which permits selective solvation and consequent dehydration at the vicinity of the peptide backbone. This provides the appropriate milieu for formation of conformations stabilized by intramolecular hydrogen bonds (*29*, *30*). The evidence for transient secondary structures in peptides in water and their subsequent stabilization by HFA and other fluoro alcohols presumably indicate the importance of secondary structure nucleation and propagation within a hydrophobic core, formed by collapse to a globular state, driven by hydrophobic effects early in the folding process.

The results of the present study establish that the dimer interface peptide C 20 may be useful as a TS inhibitor, targeted to non active site residues. It has been noted that while several inactive mutants of *E. coli* TS can be combined to yield functional heterodimers in aqueous buffers, subunits of *L. casei* or T4-phage TS do not complement one another, indicating that homologous dimers from various species can differ in subunit affinity. Moreover, mixing comparable mutants of TS from different species (*L. casei* and *E. coli* or *E. coli* and T4 phage) did not restore activity (*15*). These results tend to suggest that despite the high degree of conservation across species, stringent sequence requirements are probably a prerequisite for the formation of stable dimers of TS (*77*). It is also noteworthy that specific amino acid substitution at the interface of *E. coli* TS seems to affect the rate of subunit association (*15*). These observations suggest that species-specific inhibitors of TS can indeed be designed to specifically target a viral or parasite enzyme selectively.

The mechanism of TS inhibition by interface peptide reported in this study appears to involve peptide-promoted protein aggregation, in a manner reminiscent of that observed in a study of calcineurin (*53*). The promotion of protein aggregation by associated proteins is a feature of filamentous amyloid deposit formation in Alzheimer's disease, with the promoting factors being called "pathological chaperones" (*78*). Facilitated protein aggregation is also observed in some cases in the presence of protein disulfide isomerase, leading to what has been termed "anti-chaperone" behavior (*79*). While the detailed mechanisms by which proteins and peptides promote protein aggregation are not well understood, this phenomenon is relatively common. In the case of C 20, the sites of interaction with TS have not been established, and the possibility that the peptide serves as a "bifunctional glue" promoting TS association cannot be ruled out. While precipitation of a target protein in vivo may appear to be a less than ideal mechanism for specific enzyme inhibition, it is pertinent to note that misfolded aggregated proteins are frequently accumulated and degraded in vivo (*80*).

ACKNOWLEDGMENT

We are grateful to Prof. Dan Santi (UCSF) for providing us the synthetic and wild-type TS genes and substrates and for introducing us to thymidylate synthase. We thank Dr. David King (UC, Berkeley) for providing the electrospray mass spectra of the synthetic peptides. All the NMR studies and computational work have been performed at the Sophisticated Instruments Facility, Indian Institute of Science, Bangalore. We thank K. Gunasekaran and Janani Venkatraman for their help in preparing Figure 1. We thank K. Gunasekaran also for his help in the calculation of ASA values.

SUPPORTING INFORMATION AVAILABLE

NMR chemical shift dispersions of the interface peptides N 22, M 17, and C 20 (Tables S1−S3) (5 pages). Ordering information is given on any current masthead page.

REFERENCES

1. Carreras, C. W., and Santi, D. V. (1995) *Annu. Rev. Biochem. 64*, 721−762.
2. Eckstein, J. W., Foster, P. G., Finer-Moore, J., Wataya, Y., and Santi, D. V. (1994) *Biochemistry 33*, 15086−15094.
3. Weichsel, A., and Montfort, W. R. (1995) *Nat. Struct. Biol. 2*, 1095−1101.
4. Santi, V., McHenry, C. S., and Sommer, H. (1974) *Biochemistry 13*, 471−481.

5. Danenberg, P. V., Langenbach, R. L., and Heidelberger, C. (1974) *Biochemistry 13*, 926−933.
6. Santi, D. V., and McHenry, C. S. (1972) *Proc. Natl. Acad. Sci. U.S.A. 69*, 1855−1857.
7. Langenbach, R. J., Danenberg, P. V., and Heidelberger, C. (1972) *Biochem. Biophys. Res. Commun. 48*, 1565−1571.
8. Appelt, K., Bacquet, R., Bartlett, C., Booth, C., Freer, S., Fuhry, M., Gehring, M. R., Herrmann, S. M., Howland, E. F., Janson, C. A., Jones, T. R., Kan, C. C., Kathardekar, V., Lewis, K. K., Marzoni, G. P., Matthews, D. A., Mohr, C., Moomaw, E. W., Morse, C. A., Oatley, S. J., Ogden, R. C., Reddy, M. R., Reich, S. H., Schoettlin, W. S., Smith, W. W., Varney, M. D., Villafranca, J. E., Ward, R. W., Webber, S., Webber, S. E., Welsh, K. M., and White, J. (1991) *J. Med. Chem. 34*, 1925−1934.
9. Schoichet, B. K., Stroud, R. M., Santi, D. V., Kuntz, I. D., and Perry, K. M. (1993) *Science 259*, 1445−1450.
10. Hardy, L. W., Finer-Moore, J. S., Montfrot, W. R., Jones, M. O., Santi, D. V., and Stroud, R. M. (1987) *Science 235*, 448−455.
11. Perry, K. M., Fauman, E. B., Finer-Morre, J. S., Montfort, W. R., Maley, G. F., Maley, F., and Stroud, R. M. (1990) *Proteins: Struct., Func., Genet. 8*, 315−333.
12. Knighton, D. R., Kan, C., Howland, E., Janson, C. A., Hostomska, Z., Welsh, K. M., and Matthews, D. A. (1994) *Nat. Struct. Biol. 1*, 186−194.
13. Schiffer, C. A., Clifton, I. J., Davisson, V. J., Santi, D. V., and Stroud, R. M. (1995) *Biochemistry 34*, 16279−16287.
14. Perry, K. M., Pookanjanatavip, M., Zhao, J., Santi, D. V., and Stroud, R. A. (1992) *Protein Sci. 1*, 796−800.
15. Maley, F., Pedersen-Lane, J., and Changchien, L. (1995) *Biochemistry 34*, 1469−1474.
16. Hol, W. G. J. (1986) *Angew. Chem., Int. Ed. Engl. 25*, 767−778.
17. Dutia, B. M., Frame, M. C., Subak-Sharp, J. H., Clark, W. N., and Marsden, H. S. (1986) *Nature 321*, 439−441.
18. Schramm, H. J., Billich, A., Jaeger, E., Rucknagel, K., Arnold, G., and Schramm (1993) *Biochem. Biophys. Res. Commun. 194*, 595−600.
19. Zhang, Z., Poorman, R. A., Maggiora, L. L., Heinrikson, R. L., and Kezdy, F. J. (1991) *J. Biol. Chem. 266*, 15591−15594.
20. Haigh, A., Greaves, R., and O'Hara, P. (1990) *Nature 344*, 257−259.
21. Matthews, D. A., Appelt, K., and Oatley, S. J. (1989) *J. Mol. Biol. 205*, 449−454.
22. Matthews, D. A., Appelt, K., Oatley, S. J., and Xuong, N. (1990) *J. Mol. Biol. 214*, 923−936.
23. Dyson, H. J., Merutka, G., Waltho, J. P., Lerner, R. A., and Wright, P. E. (1992) *J. Mol. Biol. 226*, 795−817.
24. Blanco, J. F., Jimenez, M. A., Herranz, J., Rico, M., Santoro, J., and Nieto, J. L. (1993) *J. Am. Chem. Soc. 115*, 5887−5888.
25. Blanco, J. F., Rivas, G., and Serrano, L. (1994a) *Nat. Struct. Biol. 1*, 584−596.
26. Blanco, J. F., Jimenez, M. A., Pineda, A., Rico, M., Santoro, J., and Nieto, J. L. (1994b) *Biochemistry 33*, 6004−6014.
27. Searle, M. S., Williams, D. H., and Packman, L. C. (1995) *Nat. Struct. Biol. 2*, 999−1006.
28. Searle, M. S., Zerella, R., Williams, D. H., and Packman, L. C. (1996) *Protein Eng. 9*, 559−565.
29. Rajan, R., Awasthi, S. K., Bhattacharjya, S., and Balaram, P. (1997) *Biopolymers 42*, 125−128.
30. Bhattacharjya, S., and Balaram, P. (1997) *Protein Sci. 6*, 1065−1073.
31. Wahba, A. J., and Friedkin, M. (1961) *J. Biol. Chem. 236*, PC11−12.
32. Creighton, T. E. (1984) *Protein Structure and Molecular Principles*, p 14, W. H. Freeman & Company, New York.
33. Santi, D. V., McHenry, C. S., & Sommer, H. (1974) *Biochemistry 13*, 471−481.
34. Hudson, E. N., and Weber, G. (1973) *Biochemistry 12*, 4154−4161.
35. Agarwalla, S., Gokhale, R. S., Santi, D. V., and Balaram, P. (1996) *Protein Sci. 5*, 270−277.
36. Pardi, A., Billeter, M., and Wüthrich, K. (1984) *J. Mol. Biol. 180*, 741−751.
37. Wishart, D. S., Sykes, B. D., and Richards, F. M. (1991) *J. Mol. Biol. 222*, 311−333.
38. Jones, S., and Thornton, J. M. (1996) *Proc. Natl. Acad. Sci. U.S.A. 93*, 13−20.
39. Babe, L. M., Rose, J., and Craik, C. S. (1992) *Protein Sci. 1*, 1244−1253.
40. Jones, S., and Thornton, J. M. (1995) *Prog. Biophys. Mol. Biol. 63*, 31−65.
41. Janin, J., Miller, S., and Chothia, C. (1988) *J. Mol. Biol. 204*, 155−164.
42. Woody, R. W. (1985) in *The Peptides: Analysis, Synthesis, Biology* (Undenfriend, S., and Meienhofer, J., Eds.) Vol. 7, pp 16−114, Academic Press, New York.
43. Rajan, R., and Balaram, P. (1996) *Int. J. Pept. Protein Res. 48*, 328−336.
44. Luidens, M. K., Figge, J., Breese, K., and Vajda, S. (1996) *Biopolymers 39*, 367−376.
45. Vuilleumier, S., Sancho, J., Loewenthal, R., and Fersht, A. R. (1993) *Biochemistry 32*, 10303−10313.
46. Chakrabartty, A., Kortemme, T., Padmanabhan, S., and Baldwin, R. L. (1993) *Biochemistry 32*, 5560−5565.
47. Osterman, D., and Kaiser, E. T. (1985) *J. Cell. Biochem. 29*, 57−72.
48. Muga, A., Surewicz, W. K., Wong, P. T. T., and Mantsch, H. H. (1990) *Biochemistry 29*, 2925−2930.
49. Wüthrich, K. (1986) *NMR of proteins and nucleic acids*, Wiley, New York.
50. Dyson, H. J., Rance, M., Houghten, R. A., Wright, P. E., and Lerner, R. A. (1988) *J. Mol. Biol. 201*, 201−217.
51. Wagner, G., Pardi, A., and Wüthrich, K. (1983) *J. Am. Chem. Soc. 105*, 5948−5949.
52. Ramachandran, G. N., Ramakrishnan, C., and Sasisekharan, V. (1963) *J. Mol. Biol. 7*, 95−99.
53. Sikkink, R., Haddy, A., MacKelvie, S., Mertz, P., Litwiller, R., and Rusnak, F. (1995) *Biochemistry 34*, 8348−8356.
54. Fisher, A., Laub, P. B., and Cooperman, B. S. (1995) *Nat. Struct. Biol. 2*, 951−955.
55. Jaenicke, R. (1987) *Prog. Biophys. Mol. Biol. 49*, 117−237.
56. Schumann, J., and Jaenicke, R. (1993) *Eur. J. Biochem. 213*, 1225−1233.
57. Gokhale, R. S., Agarwalla, S., Santi, D. V., and Balaram, P. (1996) *Biochemistry 35*, 7150−7158.
58. Gokhale, R. S., Agarwalla, S., Francis, V. S., Santi, D. V., and Balaram, P. (1994) *J. Mol. Biol. 235*, 89−94.
59. Montfort, W. R., Perry, K. M., Fauman, E. B., Finer-Moore, J. S., Maley, G. F., Hardy, L., Maley, F., and Stroud, R. M. (1990) *Biochemistry 29*, 6964−6977.
60. Awasthi, S. K., Raghotham, S., and Balaram, P. (1995) *Biochem. Biophys. Res. Commun. 216*, 375−381.
61. Struthers, M. D., Cheng R. P., and Imperiali, B. (1996) *Science 271*, 341−344.
62. Haque, T. S., and Gellman, S. H. (1997) *J. Am. Chem. Soc 119*, 2303−2304.
63. Dyson, H. J., Satterthwait, A. C., Lerner, R. A., and Wright, P. E. (1990) *Biochemistry 29*, 7828−7837.
64. Yang, J. J., Buck, M., Pitkeathly, M., Kotik, M., Haynie, D. T., Dobson, C. M., and Radford, S. E. (1995) *J. Mol. Biol. 252*, 483−492.
65. Kemmink, J., and Creighton, T. E. (1993) *J. Mol. Biol. 234*, 861−878.
66. Kemmink, J., and Creighton, T. E. (1995) *Biochemistry 34*, 12630−12635.
67. Munoz, V., Serrano, L., Jimenez, M. A., and Rico, M. (1995) *J. Mol. Biol. 247*, 648−669.
68. Hamada, D., Kuroda, Y., Tanaka, T., and Goto, Y. (1995) *J. Mol. Biol. 254*, 737−746.
69. Sonnichsen, F. D., Van Eyk, J. E., Hodges, R. S., and Sykes, B. D. (1992) *Biochemistry 31*, 8790−8798.
70. Minor, D. L., Jr., and Kim, P. S. (1994) *Nature 367*, 660−663.

71. Smith, C. K., and Regan, L. (1995) *Science 270*, 980−982.
72. O'Neil, K. T., and Degrado, W. F. (1990) *Science 250*, 646−650.
73. Chakrabartty, A., Schellman, J. A., and Baldwin, R. L. (1991) *Nature 351*, 586−588.
74. Creighton, T. E. (1994) *Nat. Struct. Biol. 1*, 135−138.
75. Dobson, C. M. (1995) *Nat. Struct. Biol. 2*, 513−517.
76. Hua, Q., Gozani, S. N., Chance, R. E., Hoffmann, J. A., Frank, B. H., and Weiss, M. A. (1995) *Nat. Struct. Biol. 2*, 129−138.
77. Carreras, C. W., Costi, P. M., and Santi, D. V. (1994) *J. Biol. Chem. 269*, 12444−12446.
78. Ma, J., Yee, A., Brewer, H. B., Jr., Das, S., and Potter, H. (1994) *Nature 372*, 92−94.
79. Primm, T. P., Walker, K. W., and Gilbert, H. F. (1996) *J. Biol. Chem. 271*, 33664−33669.
80. Marquardt, T., and Helenius, A. (1992) *J. Cell Biol. 3*, 505−513.
81. Kraulis, P. J. (1991) *J. Appl. Crystallogr. 24*, 946−950.

BI9720989